



Published in final edited form as:

Toxicology. 2015 February 3; 328: 168–178. doi:10.1016/j.tox.2014.12.015.

Modifying welding process parameters can reduce the neurotoxic potential of manganese-containing welding fumes

Krishnan Sriram*, Gary X. Lin, Amy M. Jefferson, Samuel Stone, Aliakbar Afshari, Michael J. Keane, Walter McKinney, Mark Jackson, Bean T. Chen, Diane Schwegler-Berry, Amy Cumpston, Jared L. Cumpston, Jenny R. Roberts, David G. Frazer, and James M. Antonini
Health Effects Laboratory Division, Centers for Disease Control and Prevention, National Institute for Occupational Safety and Health, Morgantown, WV 26505, USA

Abstract

Welding fumes (WF) are a complex mixture of toxic metals and gases, inhalation of which can lead to adverse health effects among welders. The presence of manganese (Mn) in welding electrodes is cause for concern about the potential development of Parkinson's disease (PD)-like neurological disorder. Consequently, from an occupational safety perspective, there is a critical need to prevent adverse exposures to WF. As the fume generation rate and physicochemical characteristics of welding aerosols are influenced by welding process parameters like voltage, current or shielding gas, we sought to determine if changing such parameters can alter the fume profile and consequently its neurotoxic potential. Specifically, we evaluated the influence of voltage on fume composition and neurotoxic outcome. Rats were exposed by whole-body inhalation (40 mg/m³; 3 h/day × 5 d/week × 2 weeks) to fumes generated by gas–metal arc welding using stainless steel electrodes (GMA-SS) at standard/regular voltage (25 V; RVSS) or high voltage (30 V; HVSS). Fumes generated under these conditions exhibited similar particulate morphology, appearing as chain-like aggregates; however, HVSS fumes comprised of a larger fraction of ultrafine particulates that are generally considered to be more toxic than their counterparts. Paradoxically, exposure to HVSS fumes did not elicit dopaminergic neurotoxicity, as monitored by the expression of dopaminergic and PD-related markers. We show that the lack of neurotoxicity is due to reduced solubility of Mn in HVSS fumes. Our findings show promise for process control procedures in developing prevention strategies for Mn-related neurotoxicity during

*Corresponding author at: Toxicology and Molecular Biology Branch, Mailstop L-3014, CDC-NIOSH, 1095 Willowdale Road, Morgantown, WV 26505, USA. Tel.: +1 304 285 6330; fax: +1 304 285 5985. kos4@cdc.gov (K. Sriram).

Conflict of interest

The authors declare they have no proprietary, financial or personal interest of any kind or nature in any samples, products, supplies, service or company that could be construed as being a conflict of interest. This is a U.S. government work and is not subject to copyright protection or restrictions.

Author contributions

KS conceived the neurotoxicology studies, performed brain dissections, analyzed the data and wrote the paper. JMA, KS designed the experimental study. KS, GXL and AMJ conducted all neurotoxicity-related assays. AA designed and built the robotic welding system. SS, WM, MJ, DGF were involved in the design, control and operation of the robotic welding and animal inhalation exposure system. AC and JLC assisted in conducting the animal inhalation exposures. BTC and DS-B characterized the welding fume aerosols. All authors reviewed and approved the final manuscript.

Transparency document

The Transparency document associated with this article can be found in the online version.

welding; however, it warrants additional investigations to determine if such modifications can be suitably adapted at the workplace to avert or reduce adverse neurological risks.

Keywords

Manganese; Neurotoxicity; Parkinson's disease; Parkinsonism; Prevention; Welding

1. Background

According to the Occupational Outlook Handbook 2014–2015, published by U.S. Department of Labor, Bureau of Labor Statistics, an estimated 500,000 workers are employed full-time in welding operations in the United States (Bureau of Labor Statistics, U.S. Department of Labor, 2014–2015). Globally, this figure exceeds 2,000,000 workers. Welders are a heterogeneous working population, employed in a number of occupational settings that include open, well-ventilated spaces (*e.g.*, outdoors on a construction site) or confined, poorly-ventilated spaces (*e.g.*, ship hull, building crawl space and pipeline). One of the most common types of welding processes used in industry is gas–metal arc welding (GMAW). In this process, shielding gases (usually a combination of argon, helium, or carbon dioxide) are continually blown through the welding nozzle and over the arc to protect the weld from weakening due to oxidation. GMAW welding process utilizes mild, low alloy or stainless steel electrodes. Mild and low alloy steel electrodes are comprised mostly of iron (Fe) with varying amounts of manganese (Mn), while stainless steel electrodes contain chromium (Cr) and nickel (Ni), in addition to Fe and Mn (Beckett, 1996).

Welding generates a complex mixture of fine and ultrafine aerosols and gaseous by-products. The welding fume (WF) comprises an array of potentially toxic metals (*e.g.*, Fe, Mn, Cr, Ni), volatilized from the welding electrode or the flux material incorporated within the electrode. Gaseous by-products (*e.g.*, ozone, carbon monoxide) generated during welding operations originate from chemical reactions, ultraviolet irradiation of atmospheric elements or the use of shielding gases. The aerodynamic diameter of WF aerosols in the welder's breathing zone ranges from 100 nm to 1 µm (Zimmer and Biswas, 2001; Jenkins et al., 2005), which are easily respirable. The unique physicochemical characteristics of these fine and ultrafine aerosol fractions can influence their deposition within the olfactory or respiratory tracts. Physical characteristics such as, size, number, concentration, morphology and surface area can influence particle translocation and toxicity. Similarly, chemical characteristics such as solubility, elemental phase, surface composition and electronic/valence state, can influence elemental speciation, translocation and toxicological profile. Therefore, exposure to airborne WF particulates is of immense occupational concern.

An emergent concern is that exposure to WF may be associated with development of neurological dysfunction similar to Parkinson's disease (PD). Much of this apprehension has been attributed to the presence of Mn in WF consumables. Magnetic resonance imaging (MRI) of welders suspected of having neurological deficits revealed hyperintense T₁ signals in basal ganglia, including globus pallidus, striatum and midbrain (Nelson et al., 1993; Kim et al., 1999; Kim, 2004; Josephs et al., 2005). These observations are indicative of Mn accumulation in the brain. Further, there is a proposition of early-onset Parkinsonism among

welders (Racette et al., 2001, 2005; Josephs et al., 2005; Bowler et al., 2006, 2007a,b). PD is characterized by progressive neurodegeneration of nigrostriatal dopaminergic neurons. While most forms of PD are sporadic, about 10% are linked to genetic defects. Identification of single gene mutations in familial forms of PD suggests that deletions and loss-of-function mutations of specific PD susceptibility genes (*PARK* genes) are associated with early-onset Parkinsonism (Kitada et al., 1998; Abbas et al., 1999; Lucking et al., 2000; Bonifati et al., 2003; Periquet et al., 2003; Rizzu et al., 2004; Neumann et al., 2004). Indeed, our recent findings link such PD susceptibility genes to occupational risk factors like welding and suggest that interaction of PD-related genes may modulate the neurotoxic outcome of exposure to WF (Sriram et al., 2010b).

As a consequence of the neurological health risks associated with welding, an immense need is felt to reduce adverse workplace exposures to WF. Therefore, controlling fume generation using appropriate ventilation and personal protective equipment to avert adverse exposures are standard safety recommendations. Unfortunately, several welding operations are performed in confined, poorly-ventilated spaces (*e.g.*, ship hull, building crawl space and pipeline), where local exhaust ventilation is impractical or sometimes ineffective. High fume concentrations in such confined workplace conditions may increase the risk for exposure. Thus, methodologies by which WF generation rate and/or welding practices can be modified to reduce toxic workplace exposures are sought after. Here, we show that by modulating a specific welding process variable, voltage, one can significantly alter fume composition and neurotoxicological outcome.

2. Methods

2.1. Welding fume generation system

Detailed characterization of the robotic welding system available at the National Institute for Occupational Safety and Health (NIOSH, Morgantown, WV) has been published previously (Antonini et al., 2006). In brief, the WF generation system consisted of a welding power source (Power Wave 455, Lincoln Electric, Cleveland, OH), an automated, programmable six-axis robotic arm (Model 100 Bi, Lincoln Electric, Cleveland, OH), and a water-cooled arc welding torch (WC 650 amp, Lincoln Electric, Cleveland, OH). Gas metal arc welding using a stainless-steel (SS) electrode (Blue Max E308LSi wire, Lincoln Electric, Cleveland, OH) was performed on A36 carbon steel base plates. Welding was performed at two different voltage settings, standard/regular voltage (25 V; RVSS) or high voltage (30 V; HVSS), keeping current and shielding gas constant (Table 1). The shielding gas was continually delivered to the welding nozzle at an air flow rate of 20 l/min. Both welding conditions produced very good weld bead quality, indicating that the welding process conditions have potential for adaptation in the industry (Fig. 1).

A flexible trunk was positioned approximately 18 inches from the arc to collect the generated fume and transport it to the animal exposure chamber (Hazleton H-1000; Lab Products, Maywood, NJ). The generated WF was mixed with humidified HEPA-filtered air to achieve the target concentration. Chamber fume concentration, temperature, and humidity were monitored. Mass concentration in the chamber was monitored in real-time with an aerosol monitor (DataRAM, Thermo Electron Co., DR-4000, Franklin, MA). Chamber

concentrations of ozone (Ozone Analyzer, Model #450, Advanced Pollution Instrumentation, Inc., San Diego, CA) and carbon monoxide (1312 Photo-acoustic Multi-Gas Monitor, Innova Air Tech Instruments, Ballerup, Denmark) were monitored to prevent adverse exposures to test animals. Ozone and carbon monoxide levels in the animal exposure chamber were not significantly higher than background levels.

2.2. Welding fume characterization

Particle size distribution and particle morphology of the fume particulates was determined as described previously (Antonini et al., 2011). In brief, particle size distribution was determined using a Micro-Orifice Uniform Deposit Impactor (MOUDI, MSP Model 110, MSP Corporation, Shoreview, MN, USA) and a Nano-MOUDI (MSP Model 115). To determine particle morphology, fume samples from the exposure chamber were collected onto grids for electron microscopy and analyzed by field emission scanning electron microscopy (FESEM). A photomicrograph representative of the particle morphology of the RVSS and HVSS fume particulates is depicted in Fig. 2A. The particle size distribution (mass median aerodynamic diameter, MMAD) characteristics of the RVSS and HVSS fumes are depicted in Fig. 2B and C, respectively. The physicochemical characteristics of the two fume particulates is presented in Table 2.

To determine the metal composition, as well as, the ratio of water-soluble and water-insoluble metal components in the WFs, elemental analysis was carried out by inductively-coupled plasma atomic emission spectroscopy (ICP-AES). During routine animal exposures to RVSS or HVSS, WF particulate samples were collected on to PVC filters in the exposure chamber. Accurately weighed (1 mg) RVSS and HVSS fume particulate samples (in quadruplicate) were collected in 1.5 ml microfuge tubes. The samples were suspended in 1 ml of distilled water, pH 7.4, and sonicated for 1 min in a Sonifier 450 Cell Disruptor (Branson Ultrasonics, Danbury, CT) to disperse the particulates (designated as total suspension). To determine the soluble and insoluble metal components of the RVSS and HVSS fume particulates, similar sets of total suspension samples were prepared, incubated at 37 °C for 24 h and centrifuged at $16,000 \times g$ for 30 min. The entire supernatant (soluble fraction) was carefully recovered and transferred to a fresh set of 1.5 ml microfuge tubes. The pellet (insoluble fraction) was air-dried and saved. ICP-AES analysis was performed by Bureau Veritas North America, Inc., (Novi, MI) according to NIOSH method 7303 (NIOSH, 2003). The total metal composition and solubility ratios of the two WFs were calculated.

2.3. Animal exposures

Male Sprague-Dawley [Hla:(SD) CVF] rats (250–300 g) were procured from Hilltop Lab Animals (Scottsdale, PA). The rats were acclimated for at least 6 days after arrival and were housed in ventilated polycarbonate cages with Diamond Dry cellulose chips as bedding, with provision for HEPA-filtered air, irradiated Teklad 2918 diet and water *ad libitum*. The NIOSH animal facility is specific pathogen-free, environmentally controlled and accredited by the Association for Assessment and Accreditation of Laboratory Animal Care International (AAALAC). All animal procedures used during the study have been reviewed and approved by the institution's Animal Care and Use Committee.

Rats ($n = 6$ per group) were exposed by whole-body inhalation to fume particulates (40 mg/m^3 ; $3 \text{ h/day} \times 5 \text{ d/week} \times 2 \text{ weeks}$; for a total of 10 days) generated by gas–metal arc–stainless steel (GMA–SS) welding at standard/regular voltage (25 V; RVSS) or high voltage (30 V; HVSS). Control animals were exposed to filtered air under similar conditions. During exposures, food and water were withheld from the animals. Body weight was monitored before and after each exposure. No significant changes in body weight were observed. No animal exhibited any outward signs of labored breathing or respiratory distress. Respiratory rate was not significantly different from air-exposed controls.

An important objective of our ongoing research is to identify early biomarkers of dopaminergic injury, which can help identify dopaminergic neurotoxicity far before any overt pathological or behavioral deficits. Such early detection is crucial for developing any intervention or prevention strategies. To this end, we have previously shown that exposure to Mn-containing WF results in altered expression of specific PD-related genes, Uchl1 (Park5) and Dj-1 (Park7), commonly associated with early-onset forms of familial PD (Sriram et al., 2010a,b). Utilizing these molecular markers alongside tyrosine hydroxylase (Th, the rate limiting enzyme in dopamine synthesis and a marker of dopaminergic neurons) as indicators of dopaminergic injury, we intend to determine how modulating welding conditions can change the neurotoxic profile.

Animals were euthanized 1 day after the last exposure. Euthanasia was performed by administration of an intraperitoneal injection of sodium pentobarbital (Sleepaway; $>100 \text{ mg/kg}$ body weight, Fort Dodge Animal Health, Wyeth, Madison, NJ), and the animals were exsanguinated prior to collection of tissues. Immediately after euthanasia, the brains were excised and brain regions (STR, striatum; MB, midbrain) from the left and right hemispheres were dissected free-hand. Tissues from the left hemisphere were stored in RNALater[®] for isolation of RNA for real-time PCR studies. Tissues from right hemisphere were frozen at $-75 \text{ }^\circ\text{C}$ for isolation of total proteins for immunoblot analysis.

2.4. RNA Isolation, cDNA synthesis and real-time PCR

The brain tissues (STR and MB) were homogenized in Tri Reagent[®] (Molecular Research Center, Inc., Cincinnati, OH) and the aqueous phase separated with MaXtract High Density gel (Qiagen, Valencia, CA). Total RNA from the aqueous phase was then isolated using RNeasy mini spin columns (Qiagen, Valencia, CA) and concentrations were determined with a NanoDrop[®] ND-1000 UV–vis Spectrophotometer (NanoDrop Technologies, Wilmington, DE). The isolated RNA was stored at $-75 \text{ }^\circ\text{C}$ until use.

First strand cDNA synthesis was carried out using total RNA ($1 \text{ } \mu\text{g}$), random hexamers and MultiScribe[™] reverse transcriptase (High Capacity cDNA Reverse Transcription Kit Applied Biosystems, Foster City, CA) in a $20 \text{ } \mu\text{l}$ reaction. Real-time PCR amplification was performed using the 7500 Real-Time PCR System (Applied Biosystems, Foster City, CA) in combination with TaqMan[®] chemistry. Specific primers and FAM[™] dye-labeled TaqMan[®] MGB probe sets (TaqMan[®] GeneExpression Assays) were procured from Applied Biosystems (Foster City, CA) and used according to the manufacturer's recommendation. All PCR amplifications (40 cycles) were performed in a total volume of $25 \text{ } \mu\text{l}$, containing $1 \text{ } \mu\text{l}$ cDNA, $1.25 \text{ } \mu\text{l}$ of the specific TaqMan[®] Gene Expression Assay and $12.5 \text{ } \mu\text{l}$ of TaqMan[®]

Gene Expression Master mix (Applied Biosystems, Foster City, CA), respectively. Sequence detection software (version 1.7; Applied Biosystems, Foster City, CA) results were exported as tab-delimited text files and imported into Microsoft Excel for further analysis. Following normalization to β -actin, relative quantification of gene expression was performed using the comparative threshold (C_T) method as described by the manufacturer (Applied Biosystems, Foster City, CA; User Bulletin 2). The values are expressed as fold change over air-exposed controls.

2.5. Preparation of brain tissues for protein analysis

Brain tissues (STR and MB) were homogenized in T-PER tissue protein extraction reagent (Pierce Biotechnologies, Inc., Rockford, IL) containing protease inhibitors and EDTA. The homogenates were centrifuged at 9,600 g for 5 min to pellet the cell/tissue debris. The supernatant was carefully collected without disturbing the pellet. Total protein was determined according to the microbicinchoninic acid (BCA) method (Pierce Biotechnologies, Inc., Rockford, IL) using bovine serum albumin as a standard. Protein extracts were stored at -75°C until use.

2.6. Western immunoblotting

Aliquots of brain homogenates (10 μg total protein) were diluted in Laemmli sample buffer, boiled and loaded on to 10% SDS-polyacrylamide gels. Proteins then were electrophoretically resolved and transferred to 0.45 μm Immobilon-FL PVDF Membranes (Millipore, Billerica, MA). Following transfer, immunoblot analysis was performed. Briefly, membranes were blocked using Odyssey Blocking Buffer (LI-COR Biosciences, Lincoln, NE) for 1 h at room temperature, washed (1×5 min; 2×10 min) with PBST, and incubated overnight at 4°C with the primary antibodies (30–50 ng/ml primary antibody buffer) to tyrosine hydroxylase (Th, rabbit polyclonal, EMD Biosciences, Gibbstown, NJ), ubiquitin carboxy-terminal hydrolase L1 (Uchl1/Pgp9.5/Park5, rabbit polyclonal, Abcam, Cambridge, MA), oncogene Dj1 (Dj1/Park7; rabbit polyclonal, Abcam, Cambridge, MA), glial fibrillary acidic protein (Gfap, mouse monoclonal, Sigma, St. Louis, MO), α -Tubulin (Tuba, mouse monoclonal, Santa Cruz Biotechnology, Inc., Santa Cruz, CA) or peptidylprolyl isomerase A (Ppia/cyclophilin A, rabbit polyclonal, EMD Biosciences, Gibbstown, NJ). Following incubation with appropriate primary antibodies, blots were washed with PBST (1×5 min; 3×10 min) and incubated for 1 h at room temperature with appropriate IRDye 680 or 800 secondary antibodies (LI-COR Biosciences, Lincoln, NE). The membranes were protected from light to minimize any photo-bleaching of the fluorescent dyes. Membranes were washed (1×5 min; 4×10 min) in PBST, followed by washes (2×3 min) in PBS. Near-infrared fluorescence detection was performed using the Odyssey Imaging System (LI-COR Biosciences, Lincoln, NE). The fluorescent signal intensities (k counts) of the individual bands were determined and normalized to endogenous controls, Tuba (55 kDa) or Ppia (15 kDa), as appropriate.

2.7. Statistical analysis

The samples ($n = 6$ per group) generated were from separate experiments that were run for RVSS and HVSS fume particulate exposures. Each experiment had separate control (filtered

Air) group. For statistical analysis, all the control and exposed groups from the two welding methods were analyzed together for each independent variable. Data were analyzed by one-way ANOVA followed by Student's–Newman–Keuls (SNK) multiple-comparison test, using SigmaStat 3.1 statistical software (Systat Software Inc., San Jose, CA). Where data failed equal variance or normality tests, they were analyzed by one-way ANOVA on Ranks followed by SNK test. Results were considered significant at $P < 0.05$. Graphical representations are Mean \pm S.E.

3. Results

3.1. Relevance of animal exposure dose to potential human (welder) exposure at the workplace

To relate our animal exposure dose to potential exposures that welders may experience in the workplace, we utilized a mathematical calculation to determine the potential exposure scenario. The calculations made here do not account for clearance or influence of any other human confounding factors, but provide an estimate of the plausible welder exposure that our experimental paradigm mimics. The MMAD for RVSS or HVSS WF aerosols was determined to be 0.39 (GSD = 1.65) μm and 0.36 μm (GSD = 1.59), respectively (Table 2), indicating that it is in the fine particle range. At this particle size, the deposition efficiency in the laboratory rat is estimated to be 11–15% (Raabe et al., 1988; MPPD, 2010). Incorporating factors such as WF aerosol concentration (FC_{WF} ; 40 mg/m^3) used in this study, rat minute ventilation volume ($MV_{(\text{rat})}$; 300 g body weight); $0.21 \times 10^{-3} \text{ m}^3/\text{min}$; CIIT and RIVM, 2006), exposure duration (ED; 3 h/day 60 min/h) and a deposition efficiency (DE) for fine particles of 13% (median of the 11–15% reported value, as above) in the following equation,

$$DLB_{(\text{rat})} = FC_{WF} \times MV_{(\text{rat})} \times ED \times DE,$$

the daily lung burden in the rat ($DLB_{(\text{rat})}$) was estimated to be about 197 $\mu\text{g}/\text{day}$. Next, to relate the rat dosing paradigm employed in this study to workplace exposures, the equivalent WF lung burden in humans was determined using surface area of alveolar epithelium (rat = 0.4 m^2 ; human = 102 m^2) as dose metric (Stone et al., 1992). From this, the daily WF lung burden in a human (welder) was estimated to be ~50 mg/day .

Based on the metal analysis, it is evident the Mn content in the RVSS and HVSS fumes ranges between 19 to 26% with a median of ~23%. Accounting for this, the daily lung burden for Mn in the rat can be calculated as $197 \times (23/100) = 45.3 \text{ } \mu\text{g}/\text{day}$. The equivalent daily lung burden in a welder would be about 11.5 mg/day based on surface area of alveolar epithelium as dose metric. Consequently, a 10 day exposure of rats to WF aerosols at 40 mg/m^3 , as conducted in this study, will mimic a cumulative Mn lung burden of ~115 mg in a welder.

The NIOSH recommended exposure limit (REL) for Mn is 1 mg/m^3 (time-weighted average, TWA). If welder exposure were to occur at this limit of 1 mg/m^3 (TWA), then the number of days of exposure required to achieve a Mn lung burden of 115 mg in a welder, can be calculated using the following formula,

$$\text{Days of exposure} = \frac{CLB_{(\text{welder})}}{FC_{Mn} \times MV_{(\text{worker})} \times ED \times DE}$$

where, FC_{Mn} is the NIOSH REL for Mn, $CLB_{(\text{welder})}$ is the equivalent cumulative lung burden in a welder based on our animal exposure model (as calculated above), $MV_{(\text{worker})}$ is the minute ventilation rate for a reference worker (a human performing light exercise; $20 \times 10^{-3} \text{ m}^3/\text{min}$; ICRP, 1994), ED is the exposure duration assuming a 8 h work schedule ($8 \text{ h/d} \times 60 \text{ min/h}$) and DE is the deposition efficiency of particles in the pulmonary alveoli (predicted as 15% based on MMAD of $0.36\text{--}0.39 \mu\text{m}$; also see ICRP, 1994; MPPD, 2010). From this the number of days required to achieve a cumulative lung Mn deposition of 115 mg is derived as follows:

$$\text{Days of exposure} = \frac{115 \text{ mg}}{[(1 \text{ mg/m}^3) \times (20 \times 10^{-3} \text{ m}^3/\text{min}) \times (8 \text{ h/d} \times 60 \text{ min/h}) \times 0.15]}$$

$$\text{Days of exposure} = \frac{115 \text{ mg}}{[1.44]} = 79.9 \text{ or } \sim 80 \text{ days}$$

Assuming a 240 day work year, which translates to 20 work days per calendar month, the number of work months of welder exposure required to achieve a Mn lung burden of 115 mg is about 4 months. Thus, our 10 day inhalation exposure to 40 mg/m^3 WF aerosol (containing ~23% Mn) in the rodent model mimics a Mn exposure paradigm of ~4 months in a welder, when exposure occurs at the NIOSH REL of 1 mg/m^3 (TWA) for Mn.

3.2. Welding fumes generated at high voltage do not cause up-regulation of divalent metal transporter 1 (Dmt1) mRNA in dopaminergic brain areas

Dmt1 (Slc11a2, Nramp2), a metal-proton symporter, transports divalent metal ions across the plasma membrane and endosomal compartment of the cell. To determine if Dmt1 plays a role in the cellular trafficking of Mn in dopaminergic brain areas, we assayed the expression of its mRNA in the STR and MB. In rats exposed to RVSS fume particulates, an increased expression of Dmt1 mRNA was observed in the STR (1.6-fold, $P < 0.05$) and MB (1.7-fold, $P < 0.05$), one day after the last exposure (Fig. 3). However, similar exposures to HVSS fume particulates failed to induce Dmt1 expression in these regions (Fig. 3).

3.3. Welding fumes generated at high voltage do not elicit neuroinflammation or oxidative stress in dopaminergic brain areas

Neuroinflammation has been implicated in the pathogenesis of several neurodegenerative diseases, including PD (Mogi et al., 1994; Hunot et al., 2001; McGeer and McGeer, 2004) and is known to precede chemical- and WF-induced dopaminergic neurotoxicity (Sriram et al., 2006a,b, 2010a). We therefore analyzed the expression of specific proinflammatory chemokines and cytokines like, chemokine (C-C motif) ligand 2 (Ccl2, Mcp1) and tumor necrosis factor α (Tnfa) in dopaminergic brain areas after exposure to two types of fumes

particulates. Small increases in the expression of *Ccl2* mRNA was observed in the STR (1.7-fold; $P < 0.05$) and MB (1.5-fold; $P < 0.05$), one day after the last exposure to RVSS fume particulates (Fig. 4). Additionally, RVSS fume particulates induced the expression of *Tnfa* (1.7-fold; $P < 0.05$) in the STR (Fig. 5), findings consistent with our earlier reports (Sriram et al., 2002, 2006a,b). *Tnfa* expression in the MB was not altered by exposure to RVSS fume particulates (data not shown). A similar exposure to HVSS fume particulates did not elicit neuroinflammation in the STR or MB (Fig. 4).

As with neuroinflammation, oxidative stress has also been suggested to be a key mediator in the pathophysiology of experimental and human PD (Sriram et al., 1997; Jenner, 2003). Increased expression of nitric oxide synthases (Nos) can result in the production of nitric oxide and peroxynitrite radicals that can prove deleterious by causing neuronal injury. To determine if WF exposure causes oxidative injury, we examined the mRNA expression of the inducible form of nitric oxide synthase (Nos2; iNos) as an index of oxidative stress. In the brain, *Nos2* has been shown to mediate the production of nitric oxide by astroglia, microglia and invasive macrophages in response to various detrimental stimuli such as inflammation, infection or ischemia (Licinio et al., 1999; Buskila et al., 2007; Ono et al., 2010). In rats exposed to RVSS fume particulates, increased expression of *Nos2* mRNA was observed in the STR (3.9-fold, $P < 0.05$), one day after the last exposure (Fig. 5). *Nos2* expression in the MB was not altered by exposure to RVSS fume particulates (data not shown). Similar exposures to HVSS fume particulates failed to induce *Nos2* in this region (Fig. 5).

3.4. Exposure to welding fumes generated at high voltage does not alter tyrosine hydroxylase protein content in dopaminergic brain areas

Loss of tyrosine hydroxylase (Th) protein is an index of injury to the dopaminergic neurons. In rats exposed to RVSS fume particulates, a small but significant decrease in Th protein content in the dopaminergic brain areas, STR (18.7%, $P < 0.05$) and MB (46.8%, $P < 0.05$), was observed one day after last exposure (Fig. 6). However, a similar exposure to HVSS fume particulates did not alter Th protein either in STR or MB (Fig. 6).

3.5. Exposure to welding fumes generated at high voltage does not alter the expression of Park proteins in dopaminergic brain areas

In humans, loss-of-function mutations in certain *PARK* genes are associated with early-onset PD (Lucking et al., 2000; Bonifati et al., 2003; Periquet et al., 2003). In the brain, these genes are normally involved in affording neuroprotection against oxidative stress resulting from mitochondrial dysfunction. We have recently shown that Mn-containing WF cause loss of Park proteins specifically in dopaminergic brain areas (Sriram et al., 2010b). Utilizing these molecular markers as predictors of Mn-induced dopaminergic injury, we examined the neurotoxic potential of WF generated at regular and high voltages. Specifically, we examined the expression of *Uhc11* (Park5) and *Dj1* (Park7) in the STR and MB. In rats exposed to RVSS fume particulates, a small but significant decrease in Park5 (21%, $P < 0.05$) and Park7 (19%, $P < 0.05$) proteins was observed in the STR, one day after the last exposure (Fig. 7). In the MB, RVSS fume particulates caused a substantial decrease in Park5 (40.5%, $P < 0.05$) and Park7 (40.7%, $P < 0.05$) proteins, one day after the last exposure

(Fig. 7). A similar exposure to HVSS fume particulates did not alter the expression of these proteins in either STR or MB (Fig. 7).

3.6. Exposure to welding fumes generated at high voltage does not cause glial activation in the striatum

Glial cells are key players in the immune response of the brain and are activated by subtle changes in neuronal milieu following neuronal perturbation or injury (Kreutzberg, 1996; Streit et al., 1999). Assessment of glial activation can therefore serve as an index of an underlying neuronal injury. In rats exposed to RVSS fume particulates, a small but significant increase in Gfap mRNA (1.4-fold, $P < 0.05$) was observed in the STR, one day after the last exposure (Fig. 8A). A concurrent increase in Gfap protein (77.5%, $P < 0.05$) was also observed in this region (Fig. 8B). Gfap expression in the MB was not altered by exposure to RVSS fume particulates (data not shown). A similar exposure to HVSS fume particulates did not alter the expression of either Gfap mRNA or protein in the STR (Fig. 8).

3.7. Welding fumes generated at high voltage contain significantly lower amounts of soluble manganese

To understand why RVSS but not HVSS fume particulates elicited neurotoxicity, we evaluated the elemental composition of the two fumes by ICP-AES analysis. WF particulates generated by HVSS contained lower amounts of Mn (26.5% less; Fig. 9). On the other hand, marginally higher levels of copper (Cu; 40% more) and chromium (Cr; 25% more) were observed in fume particulates generated by HVSS (Fig. 9). Iron (Fe) content was not significantly altered by welding at either of the voltage conditions. We also determined the elemental composition of the insoluble and soluble fractions of the fume particulates collected following RVSS or HVSS welding. Fumes generated by HVSS welding had significantly lower soluble Mn content (84% less) as compared to that generated by RVSS (Fig. 10). A small decrease in the insoluble Mn content (29%) was also observed in fume particulates generated by HVSS welding as compared to that generated by RVSS (Fig. 10). Besides Mn, a decrease in the soluble Ni content (50% less) was also seen in fume particulates generated by HVSS but not RVSS welding. The soluble fraction of other metals like Cu, Fe or zinc (Zn) did not differ significantly between RVSS or HVSS welding conditions.

4. Discussion

Gas–metal arc welding is an important industrial process employed to coalesce metals. An inevitable consequence of arc welding is the generation of fumes that can be potentially hazardous to the welder's health. The chemical composition and particle size of the welding aerosol are important determinants of the toxicity of WF. The chemical composition and the fume formation rate are influenced by various factors, including, welding parameters and processes, filler and base materials, as well as, shielding gas combinations. Due to the high temperatures associated with arc welding, metal aerosols are thought to predominately originate from the molten tip of the welding electrode, although the molten weld pool is also a significant source. These metal aerosols immediately undergo oxidation and rapidly condense into fine and nano-sized particles. The aerodynamic diameter of WF aerosols in

the welder's breathing zone is reported to range from 100 nm to 1 μ m (Zimmer and Biswas, 2001; Jenkins et al., 2005), which are easily respirable and can deposit in the olfactory and lower respiratory tract. As ultrafine particles or the soluble metal fractions can translocate and accumulate in the brain (Hunter and Udem, 1999; Oberdörster et al., 2002, 2004; Elder et al., 2006), questions have been raised regarding a causal association between WF exposure and neurological effects seen in welders. Particularly, the presence of Mn in welding consumables is thought to be associated with the appearance of PD-like neurological manifestations. Indeed, our recent findings demonstrate that exposure to Mn-containing WF result in selective accumulation of Mn in dopaminergic brain areas and alter the expression of specific PD-related genes (Park genes) that are commonly associated with early-onset forms of familial PD (Sriram et al., 2010a,b). Changes in these markers preceded any overt pathological or behavioral deficits, suggesting that these indices could serve as early predictors of dopaminergic injury.

The fumes generated during welding are complex aerosols of gases and metals, the composition and morphology of which is influenced by the type of electrode, process variables (current, voltage, shielding gas) or the base metal on which welding is performed. Because neurological disease conditions associated with occupational and environmental exposures are generally progressive in nature, with latency between insult and appearance of clinical symptoms, a logical approach for workplace safety and health would be to prevent adverse exposures. For welding, this can be achieved by minimizing WF generation rate and/or suitably modifying existing welding practices to reduce toxic exposures. Here, we show that by specifically modulating welding voltage, keeping current and shielding gas constant, the fume composition and neurotoxicological properties of Mn-containing WF can be significantly altered.

To assess the neurotoxic effects of exposure to WF particulates generated at different voltages, we evaluated various indices of neural injury, particularly those relevant to dopaminergic neurotoxicity. These included, the dopaminergic marker Th, PD-linked (Park) proteins, neuroinflammatory mediators, markers of glial activation and a metal transporter known to facilitate uptake of divalent cations like Mn. Exposure to GMA-SS fume particulates generated at the standard/regular voltage of 25 V (RVSS) resulted in reduced expression of Th, Park5 and Park7 proteins in the striatum and midbrain, consistent with our earlier findings (Sriram et al., 2010a,b). These changes were associated with increased expression of the metal-proton symporter Dmt1 (Slc11a2, Nramp2), suggesting potential uptake of Mn into these dopaminergic targets. Indeed, we have previously shown that following exposure to WF particulates, Mn, but not other elements, is selectively taken up in to the brain (Sriram et al., 2010b). The presence of Mn in these regions, elicited an inflammatory response as determined by the expression of proinflammatory mediators like Ccl2, Tnfa and Nos2. Interestingly, GMA-SS fume particulates generated by welding at a higher voltage (30 V; HVSS) did not alter the expression of any of the neural injury markers assessed. Intrigued by this, we characterized the fume particulates generated by the two voltage conditions to understand if any of the physicochemical properties of the fume particulates may have contributed to this apparent lack of neurotoxicity. Although fume particulates generated by HVSS exhibited a greater number of ultrafine-sized particles (Antonini et al., 2011), elemental analysis revealed that the HVSS fume particulates

contained significantly lower amounts of soluble Mn. It is plausible that the difference in the neurotoxic profile of WF generated at high voltage may be due to alterations in the speciation and consequently the solubility of Mn that rendered it less toxic.

Previous studies (Hovde and Raynor, 2007) have shown that the concentration of ultrafine particles generated during gas-metal arc welding at high voltage is about three times more than that observed at a lower voltage. As the welding voltage increases, the type of metal transfer changes from short-circuit to spray-arc that affects the heat of the weld and the molten surface area (Gray and Hewitt, 1982; Hovde and Raynor, 2007). At lower voltage, the electrode short-circuits keeping the temperature low, which reduces metal vaporization and subsequent recondensation (Hovde and Raynor, 2007). During spray-arc transfer at higher voltage, the heat output can influence metal volatilization producing a greater number of ultrafine particles and likely change the metal profile of the fume.

Despite the generation of a larger amount of ultrafine metal particulates following HVSS welding, we observed that the Mn content in these fumes were lower; particularly the soluble fraction of Mn was significantly less in the HVSS fumes. It should be noted that the percent Mn content in the aerosol is not reflective of the Mn amount in the electrodes as listed by the manufacturer. In the aerosol, Mn levels are always significantly higher than that observed in the electrode. This is because Mn is known to have a substantially lower boiling point than Fe (Hovde and Raynor, 2007), which causes Mn to vaporize more readily. Consequently its presence in the WF aerosol is higher than in the original electrode on a percentage basis. It has been reported that the percentage of Mn in WF on a mass basis was 7.1% when welding was performed at a voltage of 23.5 V as compared to the 11.5% observed at 16 V. This suggests that the composition of the WF particulates is dependent on the voltage conditions (Hovde and Raynor, 2007). These findings are consistent with previous observations from our group (Keane et al., 2010) that showed higher fume generation rates, but lower Mn emission rates, when welding occurred at high voltage. At higher voltage, it is likely that more Fe is aerosolized, which can potentially alter the Fe:Mn ratio of the aerosol. Indeed, our current findings indicate the possibility of such an occurrence. At low voltage (25 V; RVSS), we observed an Fe:Mn ratio of 2:1, whereas at a high voltage (30 V; HVSS) the Fe:Mn ratio changed to 3:1, indicating the presence of more Fe. On the other hand, the ratio of Fe:Cr was not different under the two voltage conditions. At higher voltages, complexation of Fe and Mn forming spinels can occur, which could potentially influence the solubility of the complex and consequently its neurotoxic potential. This is consistent with the report that WF generated at lower voltage (30 V) exhibited a higher dopamine oxidation rate compared to that generated at higher voltage (40 V), which coincided with the increase in the ratio of Fe to Mn (Hudson et al., 2001). Based on their *in vitro* dopamine oxidation studies, Hudson et al. (2001) suggest that the voltage setting is an important factor in determining the potential neurotoxicity of WF. Our observations from *in vivo* inhalation studies that assessed various indices of dopaminergic neurotoxicity provide substantial evidence in support of this notion. Consequently, based on our observations, the lower emission rates for Mn and its reduced solubility in HVSS fumes may be responsible for the lack of neurotoxicity in animals exposed to HVSS fume particulates, perhaps due to reduced bioavailability.

The toxicity of Mn in WF can vary considerably depending on its oxidation state, biotransformation or formation of complexes with other elements. Bioavailability and bio-accessibility are key determinants of elemental uptake, which in turn is governed by the chemical speciation. Oxidation state can affect the absorption, trans-membrane transport, clearance, and toxicity at the cellular and molecular level. Redox transformations are known to alter the speciation and bioavailability of several elements, including Mn. The stable and metastable forms of Mn (3^+ and 4^+) are insoluble and are thought to be less bioavailable. However, changes in pH, oxygen, chloride and/or carbonate concentrations in local intracellular environment during normal physiological events or due to adverse effects of the exposure can potentially alter the chemical speciation and complexation of elements. Such biotransformation can result in bioavailability of soluble species and consequently toxicity. It is likely that the lung can initially act as a reservoir for such insoluble WF particulates, and gradual biotransformation and dissolution of these particles over time may render them bioavailable to extra-pulmonary targets, including the brain. The accumulation of high levels of Mn in the lungs of MMA-HS or GMA-MS fume exposed animals, but not the soluble MnCl_2 exposed animals, are suggestive of such an occurrence (Sriram et al., 2010b). Mn^{2+} , on the other hand is highly soluble, taken up rapidly by cells, and likely rapidly cleared. Indeed, less Mn was found in the lungs following exposure to a soluble Mn^{2+} salt than less soluble Mn^{3+} or Mn^{4+} salts, indicating rapid pulmonary clearance (Dorman et al., 2001). However, it must be borne in mind that Mn^{2+} is also quite susceptible to oxidation forming Mn^{3+} and Mn^{4+} , which can become bio-persistent. Transport of Mn, particularly Mn^{2+} , in the brain is mediated by divalent metal transporter 1 (Dmt1; Nramp2; Slc11a2), an important symporter for intracellular transport of divalent ions like Fe^{2+} , Mn^{2+} , Co^{2+} , Zn^{2+} , Cu^{2+} etc., but not their trivalent forms (Gunshin et al., 1997). Transferrin is responsible for transporting Mn^{3+} in the blood, while α_2 -microglobulin is thought to transport Mn^{2+} in the blood (Gibbons et al., 1976). Since the fume particulates generated by HVSS welding exhibited reduced solubility, we hypothesize there is less bioavailability that may likely have contributed to the lack of neurotoxicity. Our findings, suggest that solubility of Mn may be a key determinant for translocation and neurotoxicological outcome. What remains to be determined is whether the speciation of Mn in RVSS and HVSS fumes influences their solubility and complexation with Fe. Our ongoing characterization studies will hopefully shed light on the role of speciation in elemental solubility of RVSS and HVSS fumes.

In conclusion, our findings show that modulating welding process parameters like voltage can potentially help reduce Mn-related neurotoxicity during welding; however, it warrants additional investigations to determine the influence of other process parameter variables, such as current and shielding gas, on the fume profile. In addition, it remains to be determined, if these modifications can be suitably adapted at the workplace to avert or reduce adverse neurological risks.

Acknowledgement

This work was funded by a NIOSH intramural grant (NIOSH ID# 9782ZBDH) to K.S.

Abbreviations

ANOVA	analysis of variance
Ccl2	chemokine (C–C motif) ligand 2
cDNA	complementary deoxyribonucleic acid
Cu	copper
Dmt1	divalent metal transporter 1
Fe	iron
FESEM	field emission scanning electron microscopy
Gfap	glial fibrillary acidic protein
GMA-SS	gas metal arc stainless steel welding
HVSS	high voltage stainless steel fume particulates
ICP-AES	inductively-coupled plasma atomic emission spectroscopy
MMAD (GSD)	mass median aerodynamic diameter (geometric standard deviation)
Mn	manganese
MB	midbrain
MOUDI	micro-orifice uniform deposit impactor
MRI	magnetic resonance imaging
mRNA	messenger ribonucleic acid
Ni	nickel
Nos2	nitric oxide synthase 2 (inducible nitric oxide synthase or iNos)
OB	olfactory bulb
Park5	Parkinson disease (autosomal dominant) 5 (also known as Uchl1, ubiquitin C-terminal hydrolase L1)
Park7	Parkinson disease (autosomal recessive, early onset) 7 (also known as Dj1)
Ppia	Peptidylprolyl isomerase A (also known as cyclophilin A)
PCR	polymerase chain reaction
PD	Parkinson's disease
RNA	ribonucleic acid
RVSS	regular voltage stainless steel fume particulates
STR	striatum
Th	tyrosine hydroxylase
T-PER	tissue protein extraction reagent

TLV-TWA	threshold limit value-time weighted average
Tnfa	tumor necrosis factor alpha
Tuba	alpha tubulin
WF	welding fume
Zn	zinc

References

- Abbas N, Lucking CB, Ricard S, Durr A, Bonifati V, De Michele G, Bouley S, Vaughan JR, Gasser T, Marconi R, Broussolle E, Brefel-Courbon C, Harhangi BS, Oostra BA, Fabrizio E, Bohme GA, Pradier L, Wood NW, Filla A, Meco G, Deneffe P, Agid Y, Brice A. A wide variety of mutations in the parkin gene are responsible for autosomal recessive parkinsonism in Europe. French Parkinson's Disease Genetics Study Group and the European Consortium on Genetic Susceptibility in Parkinson's Disease. *Hum. Mol. Genet.* 1999; 8:567–574. [PubMed: 10072423]
- Antonini JM, Afshari AA, Stone S, Chen B, Schwegler-Berry D, Fletcher WG, Goldsmith WT, Vandestouwe KH, McKinney W, Castranova V, Frazer DG. Design, construction, and characterization of a novel robotic welding fume generator and inhalation exposure system for laboratory animals. *J. Occup. Environ Hyg.* 2006; 3(4):194–203. [PubMed: 16531292]
- Antonini JM, Keane M, Chen BT, Stone S, Roberts JR, Schwegler-Berry D, Andrews RN, Frazer DG, Sriram K. Alterations in welding process voltage affect the generation of ultrafine particles, fume composition, and pulmonary toxicity. *Nanotoxicology.* 2011; 5(4):700–710. [PubMed: 21281223]
- Beckett, WS. Welding. In: Harber, P.; Schenker, MB.; Balmes, JR., editors. *Occupational and Environmental Respiratory Disease.* Mosby-Year Book, Inc.; St. Louis, MO: 1996. p. 704-717.
- Bonifati V, Rizzu P, van Baren MJ, Schaap O, Breedveld GJ, Krieger E, Dekker MC, Squitieri F, Ibanez P, Joosse M, van Dongen JW, Vanacore N, van Swieten JC, Brice A, Meco G, van Duijn CM, Oostra BA, Heutink P. Mutations in the DJ-1 gene associated with autosomal recessive early-onset parkinsonism. *Science.* 2003; 299:256–259. [PubMed: 12446870]
- Bowler RM, Gysens S, Diamond E, Nakagawa S, Drezgic M, Roels HA. Manganese exposure: neuropsychological and neurological symptoms and effects in welders. *Neurotoxicology.* 2006; 27:315–326. [PubMed: 16343629]
- Bowler RM, Nakagawa S, Drezgic M, Roels HA, Park RM, Diamond E, Mergler D, Bouchard M, Bowler RP, Koller W. Sequelae of fume exposure in confined space welding: a neurological and neuropsychological case series. *Neurotoxicology.* 2007a; 28:298–311. [PubMed: 17169432]
- Bowler RM, Roels HA, Nakagawa S, Drezgic M, Diamond E, Park R, Koller W, Bowler RP, Mergler D, Bouchard M, Smith D, Gwiazda R, Doty RL. Dose-effect relationships between manganese exposure and neurological: neuropsychological and pulmonary function in confined space bridge welders. *Occup. Environ. Med.* 2007b; 64:167–177. [PubMed: 17018581]
- Bureau of Labor Statistics, U.S. Department of Labor. [accessed: 03.20.2014] Occupational Outlook Handbook Welders, Cutters, Solderers, and Brazers. 2014–2015. <http://www.bls.gov/ooh/production/welders-cutters-solderers-and-brazers.htm#tab-1>
- Buskila Y, Abu-Ghanem Y, Levi Y, Moran A, Grauer E, Amitai Y. Enhanced astrocytic nitric oxide production and neuronal modifications in the neocortex of a NOS2 mutant mouse. *PLoS One.* 2007; 2(9):e843. [PubMed: 17786214]
- CIIT. RIVM. Multiple Path Particle Dosimetry Model (MPPD, version 2.0): A Model for Human and Rat Airway Particle Dosimetry. Centers for Health Research (CIIT); Research Triangle Park, NC: 2006.
- Dorman DC, Struve MF, James RA, Marshall MW, Parkinson CU, Wong BA. Influence of particle solubility on the delivery of inhaled manganese to the rat brain: manganese sulfate and manganese tetroxide pharmacokinetics following repeated (14-day) exposure. *Toxicol. Appl. Pharmacol.* 2001; 170(2):79–87. [PubMed: 11162771]

- Elder A, Gelein R, Silva V, Feikert T, Opanashuk L, Carter J, Potter R, Maynard A, Ito Y, Finkelstein J, Oberdorster G. Translocation of inhaled ultrafine manganese oxide particles to the central nervous system. *Environ. Health Perspect.* 2006; 114:1172–1178. [PubMed: 16882521]
- Gibbons RA, Dixon SN, Hallis K, Russell AM, Sansom BF, Symonds HW. Manganese metabolism in cows and goats. *Biochim. Biophys. Acta.* 1976; 444(1):1–10. [PubMed: 60137]
- Gray CN, Hewitt PJ. Control of particulate emissions from electric-arc welding by process modification. *Ann. Occup. Hyg.* 1982; 25:431–438. [PubMed: 7165223]
- Gunshin H, Mackenzie B, Berger UV, Gunshin Y, Romero MF, Boron WF, Nussberger S, Gollan JL, Hediger MA. Cloning and characterization of a mammalian proton-coupled metal-ion transporter. *Nature.* 1997; 388(6641):482–488. [PubMed: 9242408]
- Hovde CA, Raynor PC. Effects of voltage and wire feed speed on weld fume characteristics. *J. Occup. Environ. Hyg.* 2007; 4:903–912. [PubMed: 17957560]
- Hudson NJ, Evans AT, Yeung CK, Hewitt PJ. Effect of process parameters upon the dopamine and lipid peroxidation activity of selected MIG welding fumes as a marker of potential neurotoxicity. *Ann. Occup. Hyg.* 2001; 45(3):187–192. [PubMed: 11295141]
- Hunot S, Hartmann A, Hirsch EC. The inflammatory response in the Parkinson brain. *Clin. Neurosci. Res.* 2001; 1:434–443.
- Hunter DD, Udem BJ. Identification and substance P content of vagal afferent neurons innervating the epithelium of the guinea pig trachea. *Am. J. Respir. Crit. Care Med.* 1999; 159:1943–1948. [PubMed: 10351943]
- ICRP. Human respiratory tract model for radiological protection: a report of a task group of the international commission on radiological protection. *Ann. ICRP.* 1994; 24(1-3):267–272.
- Jenkins NT, Pierce WM-G, Eagar TW. Particle size distribution of gas metal and flux cored arc welding fumes. *Weld. J.* 2005; 84:156S–163S.
- Jenner P. Oxidative stress in Parkinson's disease. *Ann. Neurol.* 2003; 53(Suppl. 3):S26–36. [PubMed: 12666096]
- Josephs KA, Ahlskog JE, Klos KJ, Kumar N, Fealey RD, Trenerry MR, Cowl CT. Neurologic manifestations in welders with pallidal MRI T1 hyperintensity. *Neurology.* 2005; 64:2033–2039. [PubMed: 15888601]
- Keane M, Stone S, Chen B. Welding fumes from stainless steel gas metal arc processes contain multiple manganese chemical species. *J. Environ. Monit.* 2010; 12:1133–1140. [PubMed: 21491680]
- Kim Y, Kim KS, Yang JS, Park IJ, Kim E, Jin Y, Kwon KR, Chang KH, Kim JW, Park SH, Lim HS, Cheong HK, Shin YC, Park J, Moon Y. Increase in signal intensities on T1-weighted magnetic resonance images in asymptomatic manganese exposed workers. *Neurotoxicology.* 1999; 20:901–907. [PubMed: 10693971]
- Kim Y. High signal intensities on T1-weighted MRI as a biomarker of exposure to manganese. *Ind. Health.* 2004; 42(2):111–115. [PubMed: 15128159]
- Kitada T, Asakawa S, Hattori N, Matsumine H, Yamamura Y, Minoshima S, Yokochi M, Mizuno Y, Shimizu N. Mutations in the parkin gene cause autosomal recessive juvenile parkinsonism. *Nature.* 1998; 392:605–608. [PubMed: 9560156]
- Kreutzberg GW. Microglia: a sensor for pathological events in the CNS. *Trends Neurosci.* 1996; 19:312–318. [PubMed: 8843599]
- Licinio J, Prolo P, McCann SM, Wong ML. Brain iNOS: current understanding and clinical implications. *Mol. Med. Today.* 1999; 5(5):225–232. [PubMed: 10322315]
- Lucking CB, Durr A, Bonifati V, Vaughan J, De Michele G, Gasser T, Harhangi BS, Meco G, Deneffe P, Wood NW, Agid Y, Brice A. Association between early-onset Parkinson's disease and mutations in the parkin gene. *New Engl. J. Med.* 2000; 342:1560–1567. [PubMed: 10824074]
- McGeer PL, McGeer EG. Inflammation and neurodegeneration in Parkinson's disease. *Parkinsonism Relat. Disord.* 2004; 10(Suppl. 1):S3–S7. [PubMed: 15109580]
- Mogi M, Harada M, Riederer P, Narabayashi H, Fujita K, Nagatsu T. Tumor necrosis factor-alpha increases both in brain and in the cerebrospinal fluid from parkinsonian patients. *Neurosci. Lett.* 1994; 165:208–210. [PubMed: 8015728]

- MPPD. Multiple-path Particle Dosimetry Model, Version 2.11. Applied Research Associates, Inc.; Albuquerque, NM: 2010. p. 2010<http://www.ara.com/products/mppd.htm>
- Nelson K, Golnick J, Korn T, Angle C. Manganese encephalopathy: utility of early magnetic resonance imaging. *Br. J. Ind. Med.* 1993; 50(6):510–513. [PubMed: 8329316]
- Neumann M, Muller V, Gorner K, Kretschmar HA, Haass C, Kahle PJ. Pathological properties of the Parkinson's disease-associated protein DJ-1 in alpha-synucleinopathies and tauopathies: relevance for multiple system atrophy and Pick's disease. *Acta Neuropathol.* 2004; 107:489–496. [PubMed: 14991385]
- NIOSH. Elements by ICP (nitric/perchloric acid ashing): method 7300. In: NIOSH. , editor. NIOSH Manual of Analytical Methods (NMAM), 3. 4th ed.. NIOSH; 2003.
- Oberdörster G, Sharp Z, Atudorei V, Elder A, Gelein R, Lunts A, Kreyling W, Cox C. Extrapulmonary translocation of ultrafine carbon particles following whole-body inhalation exposure of rats. *J. Toxicol. Environ. Health A.* 2002; 65:1531–1543. [PubMed: 12396867]
- Oberdorster G, Sharp Z, Atudorei V, Elder A, Gelein R, Kreyling W, Cox C. Translocation of inhaled ultrafine particles to the brain. *Inhal. Toxicol.* 2004; 16:437–445. [PubMed: 15204759]
- Ono K, Suzuki H, Sawada M. Delayed neural damage is induced by iNOS-expressing microglia in a brain injury model. *Neurosci. Lett.* 2010; 473(2):146–150. [PubMed: 20178828]
- Periquet M, Latouche M, Lohmann E, Rawal N, De Michele G, Ricard S, Teive H, Fraix V, Vidailhet M, Nicholl D, Barone P, Wood NW, Raskin S, Deleuze JF, Agid Y, Durr A, Brice A. Parkin mutations are frequent in patients with isolated early-onset parkinsonism. *Brain.* 2003; 126:1271–1278. [PubMed: 12764050]
- Raabe OG, Al-Bayati MA, Teague SV, Rasolt A. Regional deposition of inhaled monodisperse coarse and fine aerosol particles in small laboratory animals. *Ann. Occup. Hyg.* 1988; 32:53–63.
- Racette BA, McGee-Minnich L, Moerlein SM, Mink JW, Videen TO, Perlmutter JS. Welding-related parkinsonism: clinical features, treatment, and pathophysiology. *Neurology.* 2001; 56:8–13. [PubMed: 11148228]
- Racette BA, Tabbal SD, Jennings D, Good L, Perlmutter JS, Evanoff B. Prevalence of parkinsonism and relationship to exposure in a large sample of Alabama welders. *Neurology.* 2005; 64:230–235. [PubMed: 15668418]
- Rizzu P, Hinkle DA, Zhukareva V, Bonifati V, Severijnen LA, Martinez D, Ravid R, Kamphorst W, Eberwine JH, Lee VM, Trojanowski JQ, Heutink P. DJ-1 colocalizes with tau inclusions: a link between parkinsonism and dementia. *Ann. Neurol.* 2004; 55:113–118. [PubMed: 14705119]
- Sriram K, Pai KS, Boyd MR, Ravindranath V. Evidence for generation of oxidative stress in brain by MPTP: in vitro and in vivo studies in mice. *Brain Res.* 1997; 749:44–52. [PubMed: 9070626]
- Sriram K, Matheson JM, Benkovic SA, Miller DB, Luster MI, O'Callaghan JP. Mice deficient in TNF receptors are protected against dopaminergic neurotoxicity: implications for Parkinson's disease. *FASEB J.* 2002; 16:1474–1476. [PubMed: 12205053]
- Sriram K, Miller DB, O'Callaghan JP. Minocycline attenuates microglial activation but fails to mitigate striatal dopaminergic neurotoxicity: role of tumor necrosis factor-alpha. *J. Neurochem.* 2006a; 96:706–718. [PubMed: 16405514]
- Sriram K, Matheson JM, Benkovic SA, Miller DB, Luster MI, O'Callaghan JP. Deficiency of TNF receptors suppresses microglial activation and alters the susceptibility of brain regions to MPTP-induced neurotoxicity: role of TNF-alpha. *FASEB J.* 2006b; 20:670–682. [PubMed: 16581975]
- Sriram K, Lin GX, Jefferson AM, Roberts JR, Chapman RS, Chen BT, Soukup JM, Ghio AJ, Antonini JM. Dopaminergic neurotoxicity following pulmonary exposure to manganese-containing welding fumes. *Arch. Toxicol.* 2010a; 84:521–540. [PubMed: 20224926]
- Sriram K, Lin GX, Jefferson AM, Roberts JR, Wirth O, Hayashi Y, Krajnak KM, Soukup JM, Ghio AJ, Reynolds SH, Castranova V, Munson AE, Antonini JM. Mitochondrial dysfunction and loss of Parkinson's disease-linked proteins contribute to neurotoxicity of manganese-containing welding fumes. *FASEB J.* 2010b; 24(12):4989–5002. [PubMed: 20798247]
- Stone KC, Mercer RR, Gehr P, Stockstill B, Crapo JD. Allometric relationships of cell numbers and size in the mammalian lung. *Am. J. Respir. Cell Mol. Biol.* 1992; 6(2):235–243. [PubMed: 1540387]

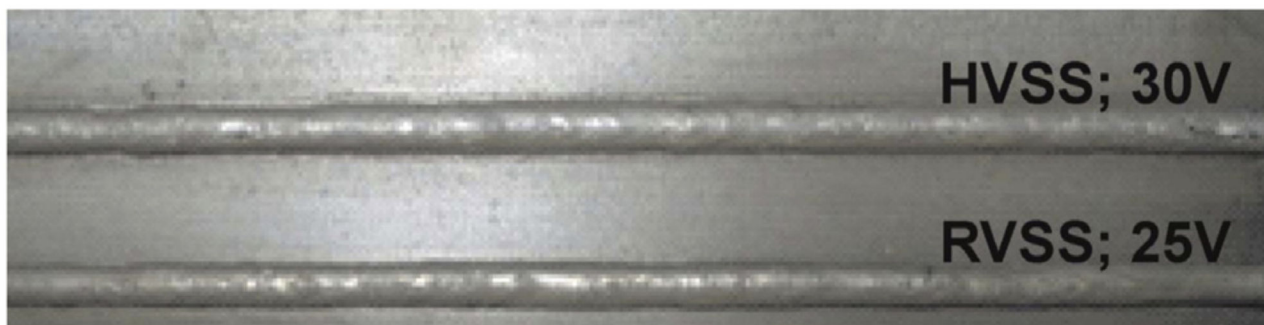
- Streit WJ, Walter SA, Pennell NA. Reactive microgliosis. *Prog. Neurobiol.* 1999; 57:563–581. [PubMed: 10221782]
- Zimmer AT, Biswas P. Characterization of the aerosols resulting from arc welding processes. *J. Aerosol Sci.* 2001; 32:993–1008.

Author Manuscript

Author Manuscript

Author Manuscript

Author Manuscript



Good weld bead quality can be achieved at regular or high voltage welding conditions

Fig.1.

Weld bead quality following GMA-SS welding at regular or high voltage. Gas-metal arc welding using a stainless-steel (SS) electrode was performed on A36 carbon steel base plates. Welding was performed at two different voltage settings, standard/regular voltage (25 V; RVSS) or high voltage (30 V; HVSS), keeping current and shielding gas constant. Note that both welding conditions produced very good weld bead quality, indicating their suitability for adaptation by the industry.

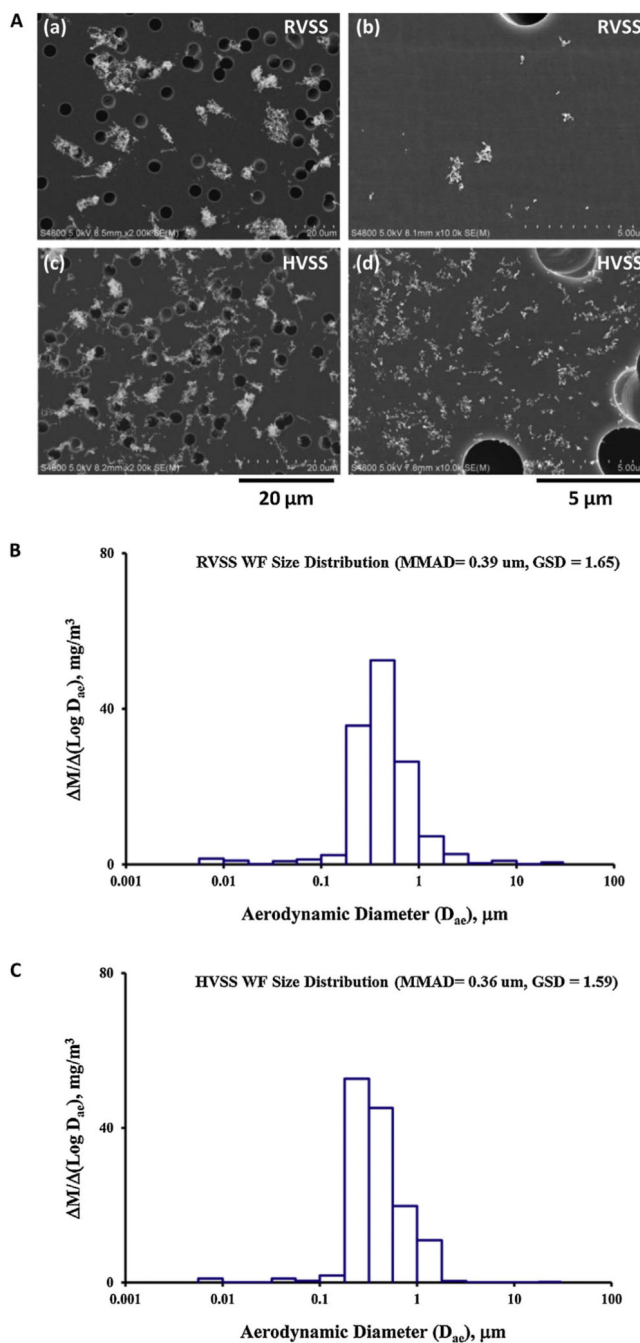


Fig. 2. (A) Scanning electron microscopy (SEM) analysis of fume particulates generated by RVSS or HVSS welding. (a and c) Fume particles collected on filters at stage 7 (particle size cut-off = 0.56 μm) of a MOUDI particle sizer. Note the similarity in particle morphology between the two process modes. (b and d) Fume particles collected on filters at stage 10 (particle size cut-off = 0.1 μm). Note the increase in ultrafine particle fraction following HVSS welding (in d). (B and C) Particle size distribution was determined using a Micro-Orifice Uniform Deposit Impactor (MOUDI) and a Nano-MOUDI. The mass median

aerodynamic diameter (MMAD) of RVSS fumes was 0.39 μm with a geometric standard deviation (GSD) of 1.65. Similarly, the MMAD of HVSS fumes was 0.36 μm with a GSD of 1.59.

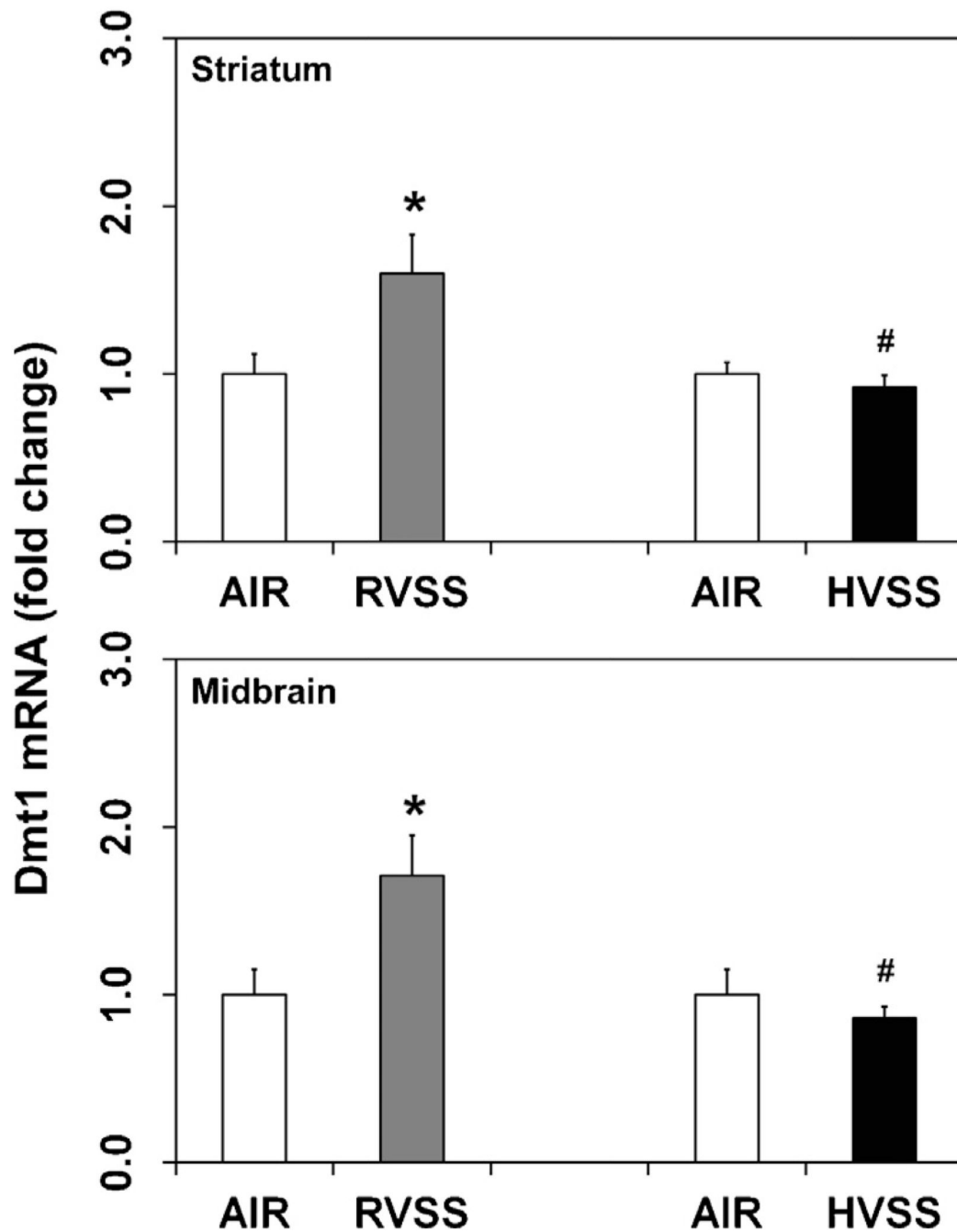


Fig. 3. Effect of RVSS and HVSS fume particulates on Dmt1 gene expression in dopaminergic brain areas. Rats were exposed by whole-body inhalation (40 mg/m^3 ; $3 \text{ h/day} \times 5 \text{ d/week} \times 2 \text{ weeks}$; for a total of 10 days) to fume particulates generated by gas-metal arc-stainless steel (GMA-SS) welding at standard/regular voltage (25 V; RVSS) or at high voltage (30 V; HVSS). At 1 day post-exposure, the mRNA expression of Dmt1 was assayed in the striatum and midbrain by TaqMan[®] real-time PCR. Following normalization to the endogenous control beta actin (Actb), the values are expressed as fold change from air-exposed controls.

Graphical representations are Mean \pm SE ($n = 6/\text{group}$). * indicates significant change from corresponding air-exposed control ($P < 0.05$). # indicates significantly different from RVSS group.

Author Manuscript

Author Manuscript

Author Manuscript

Author Manuscript

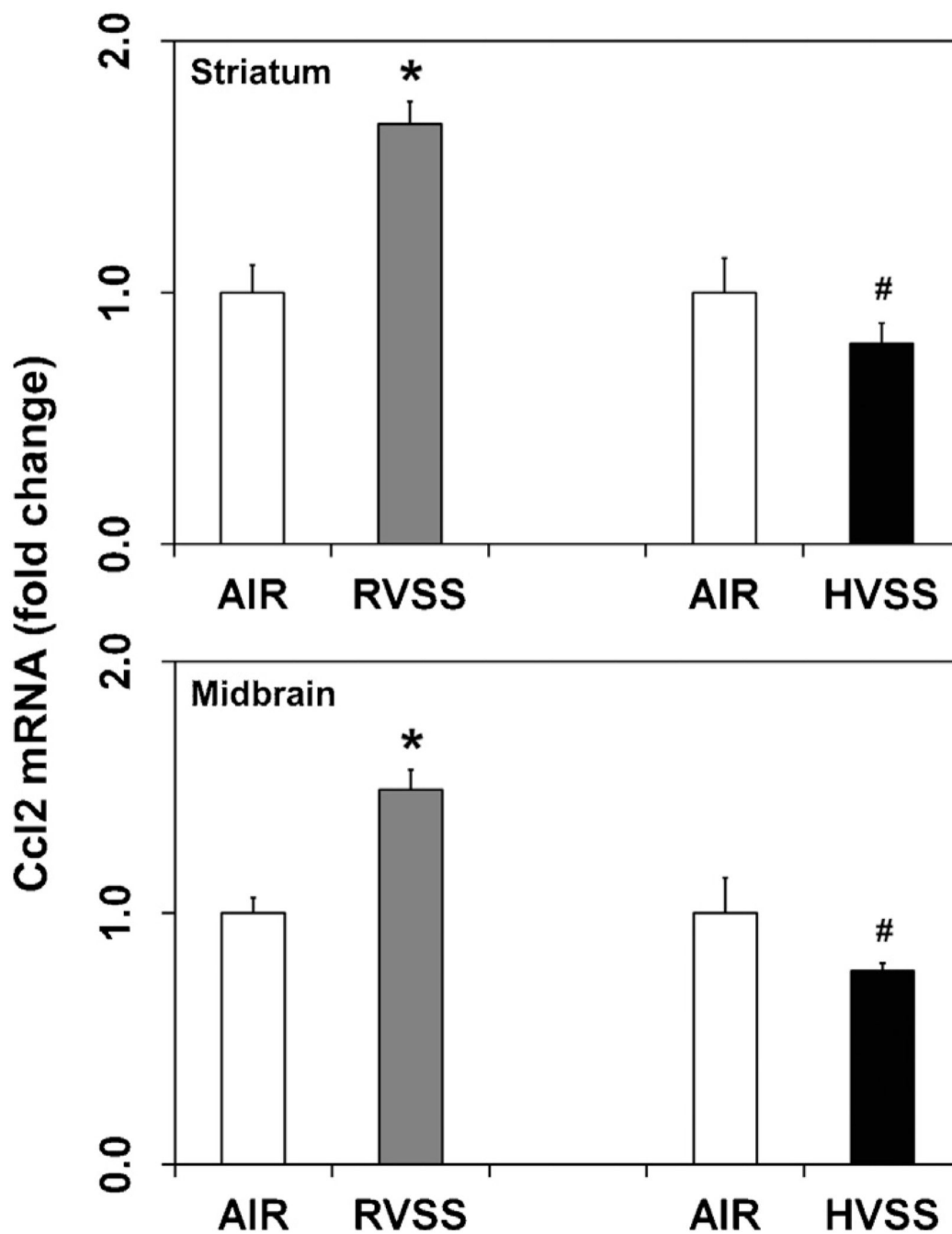


Fig. 4. Effect of RVSS and HVSS fume particulates on Ccl2 gene expression in dopaminergic brain areas. Rats were exposed by whole-body inhalation (40 mg/m^3 ; 3 h/day \times 5 d/week \times 2 weeks; for a total of 10 days) to fume particulates generated by gas-metal arc-stainless steel (GMA-SS) welding at standard/regular voltage (25 V; RVSS) or at high voltage (30 V; HVSS). At 1 day post-exposure, the mRNA expression of Ccl2 was assayed in the striatum and midbrain by TaqMan[®] real-time PCR. Following normalization to the endogenous control beta actin (Actb), the values are expressed as fold change from air-exposed controls.

Graphical representations are Mean \pm SE ($n = 6/\text{group}$). * indicates significant change from corresponding air-exposed control ($P < 0.05$). # indicates significantly different from RVSS group.

Author Manuscript

Author Manuscript

Author Manuscript

Author Manuscript

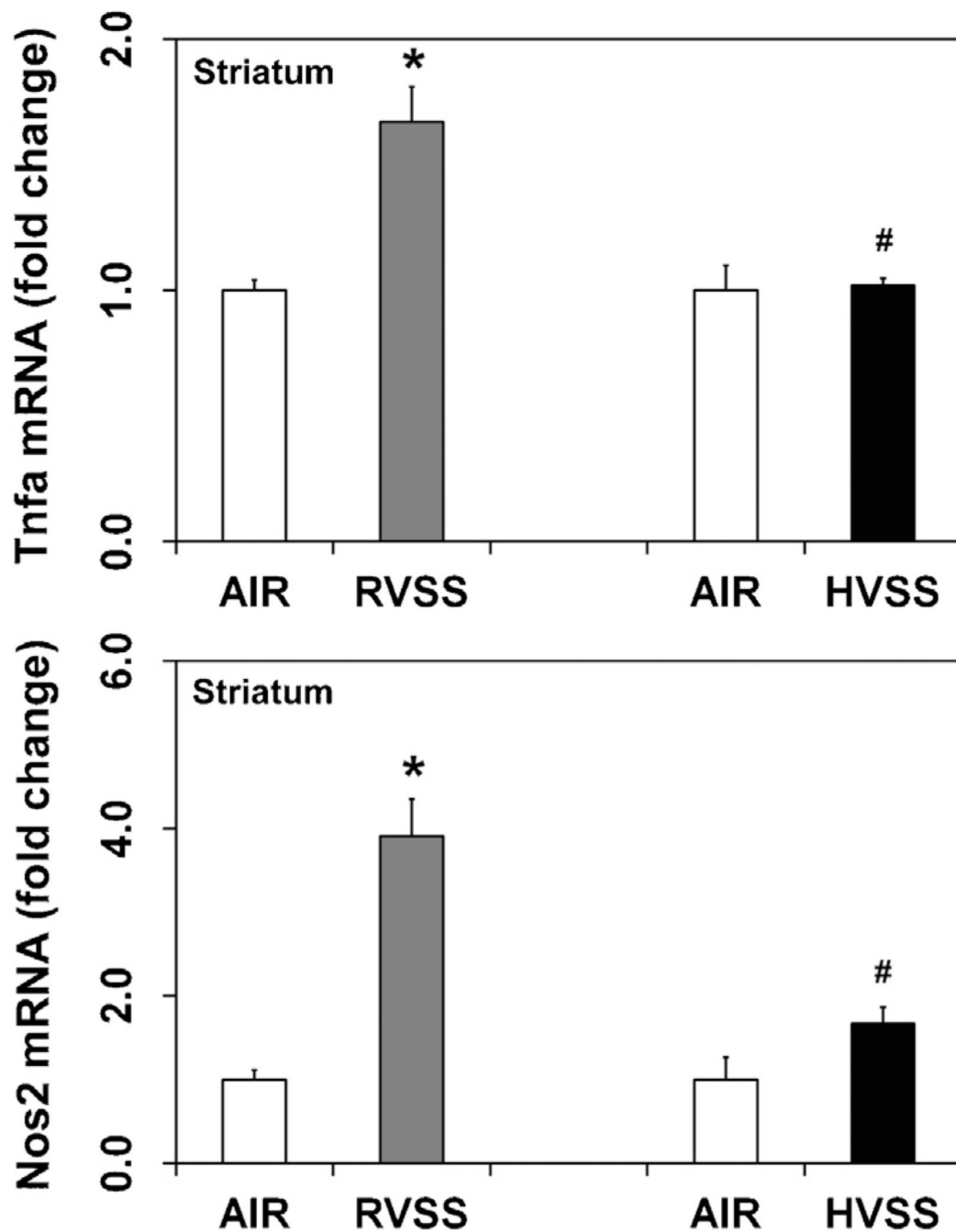


Fig. 5. Effect of RVSS and HVSS fume particulates on Tnfa and Nos2 gene expression in the striatum. Rats were exposed by whole-body inhalation (40 mg/m^3 ; 3 h/day \times 5 d/week \times 2 weeks; for a total of 10 days) to fume particulates generated by gas-metal arc-stainless steel (GMA-SS) welding at standard/regular voltage (25 V; RVSS) or at high voltage (30 V; HVSS). At 1 day post-exposure, the mRNA expression of Tnfa and Nos2 was assayed in the striatum by TaqMan[®] real-time PCR. Following normalization to the endogenous control beta actin (Actb), the values are expressed as fold change from air-exposed controls.

Graphical representations are Mean \pm SE ($n = 6/\text{group}$). * indicates significant change from corresponding air-exposed control ($P < 0.05$). # indicates significantly different from RVSS group.

Author Manuscript

Author Manuscript

Author Manuscript

Author Manuscript

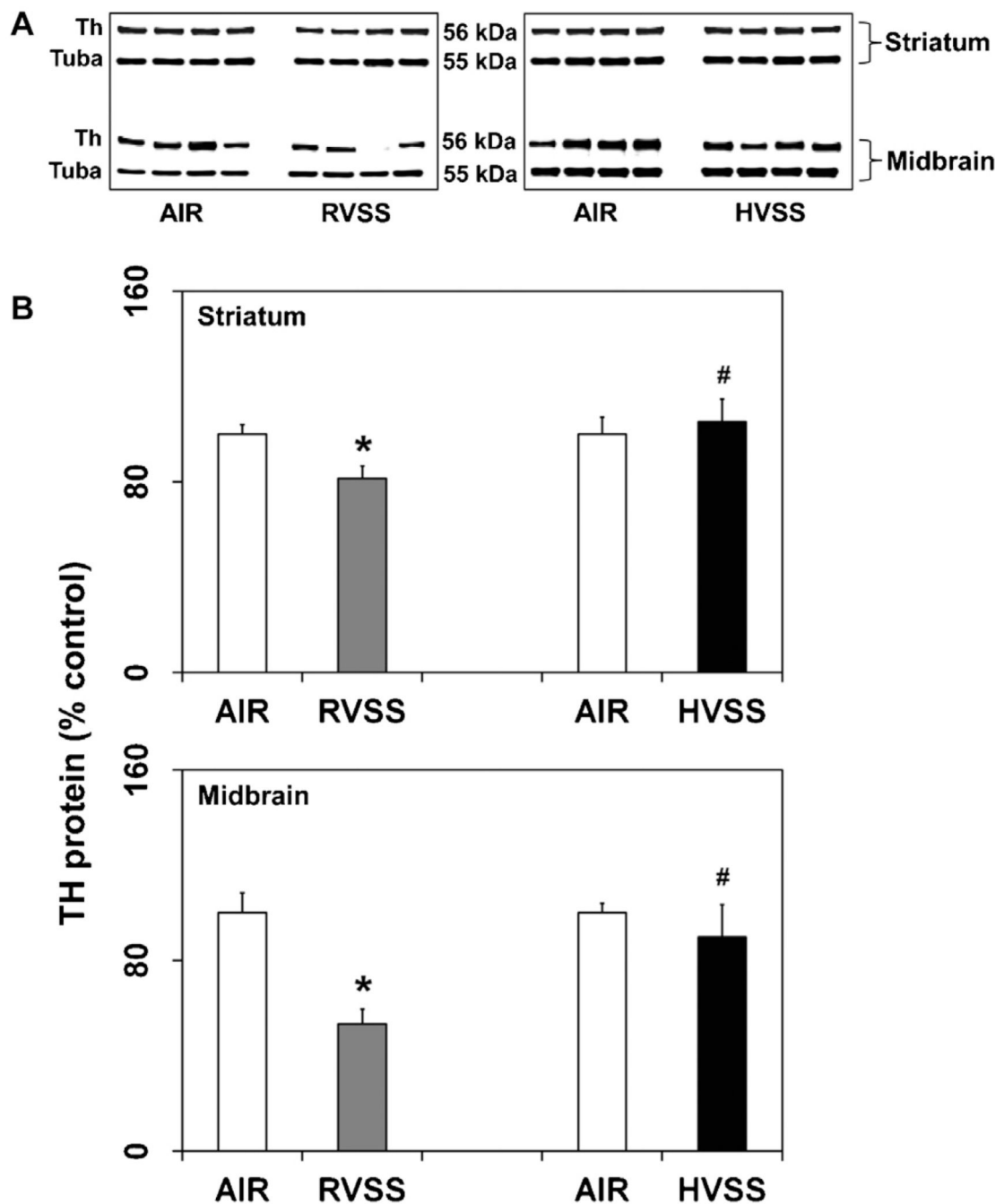


Fig. 6. Effect of RVSS and HVSS fume particulates on tyrosine hydroxylase protein expression in dopaminergic brain areas. Rats were exposed by whole-body inhalation (40 mg/m^3 ; 3 h/day \times 5 d/week \times 2 weeks; for a total of 10 days) to fume particulates generated by gas-metal arc-stainless steel (GMA-SS) welding at standard/regular voltage (25 V; RVSS) or at high voltage (30 V; HVSS). (A) At 1 day post-exposure, the expression of Th protein was determined by immunoblot analysis in the STR and MB. (B) Following normalization to the endogenous control alpha tubulin (Tuba), the values are expressed as percent of air-exposed

controls. Graphical representations are Mean \pm SE ($n = 4/\text{group}$). * indicates significant change from corresponding air-exposed control ($P < 0.05$). # indicates significantly different from RVSS group.

Author Manuscript

Author Manuscript

Author Manuscript

Author Manuscript

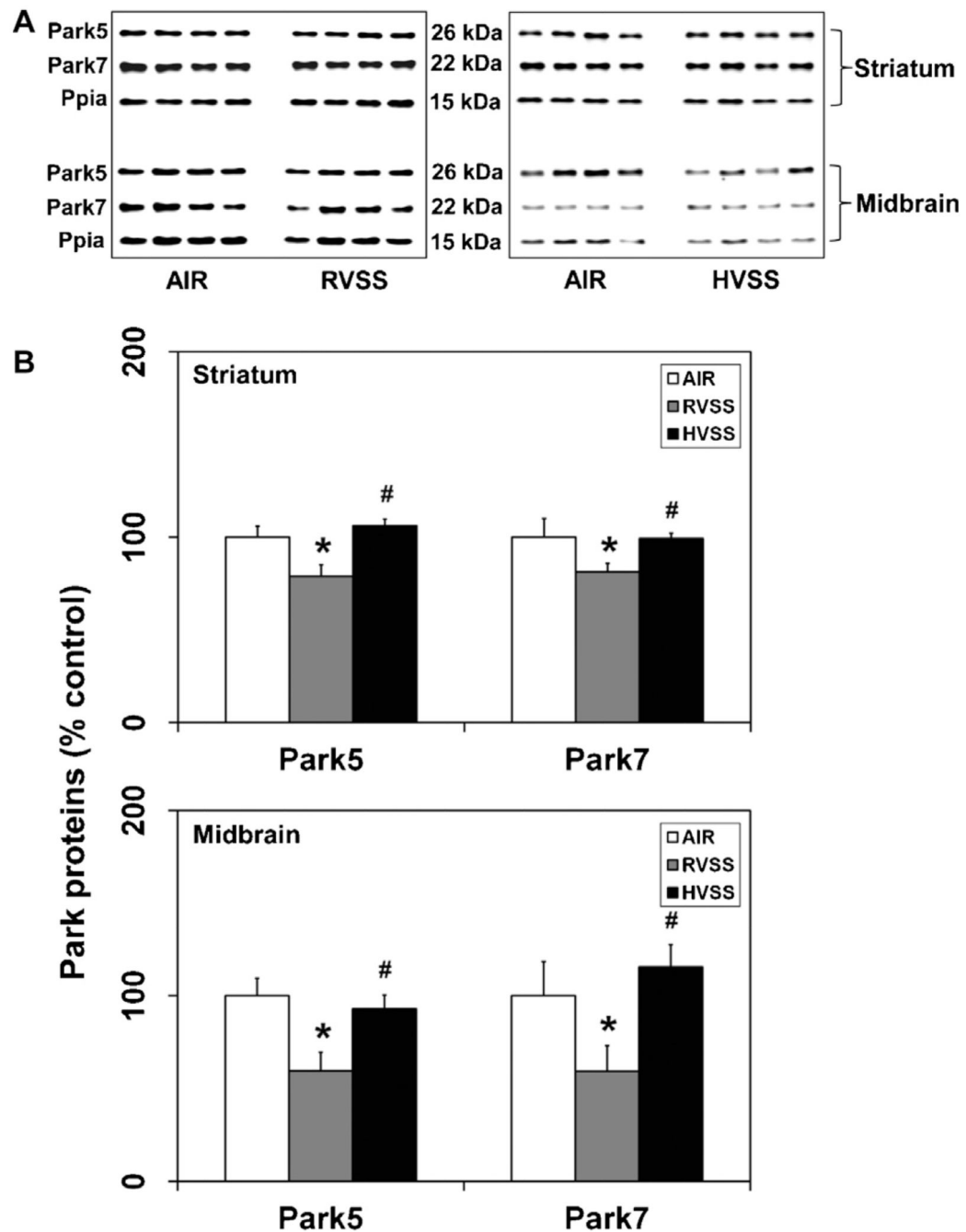


Fig. 7. Effect of RVSS and HVSS fume particulates on the expression of PD-related markers in dopaminergic brain areas. Rats were exposed by whole-body inhalation (40 mg/m^3 ; 3 h/day \times 5 d/week \times 2 weeks; for a total of 10 days) to fume particulates generated by gas-metal arc-stainless steel (GMA-SS) welding at standard/regular voltage (25 V; RVSS) or at high voltage (30 V; HVSS). (A) At 1 day post-exposure, the expression of Park5 and Park7 proteins were determined by immunoblot analysis in the STR and MB. (B) Following normalization to the endogenous control cyclophilin A (Ppia), the values are expressed as

percent of air-exposed controls. Graphical representations are Mean \pm SE ($n = 4/\text{group}$). * indicates significant change from corresponding air-exposed control ($P < 0.05$). # indicates significantly different from RVSS group.

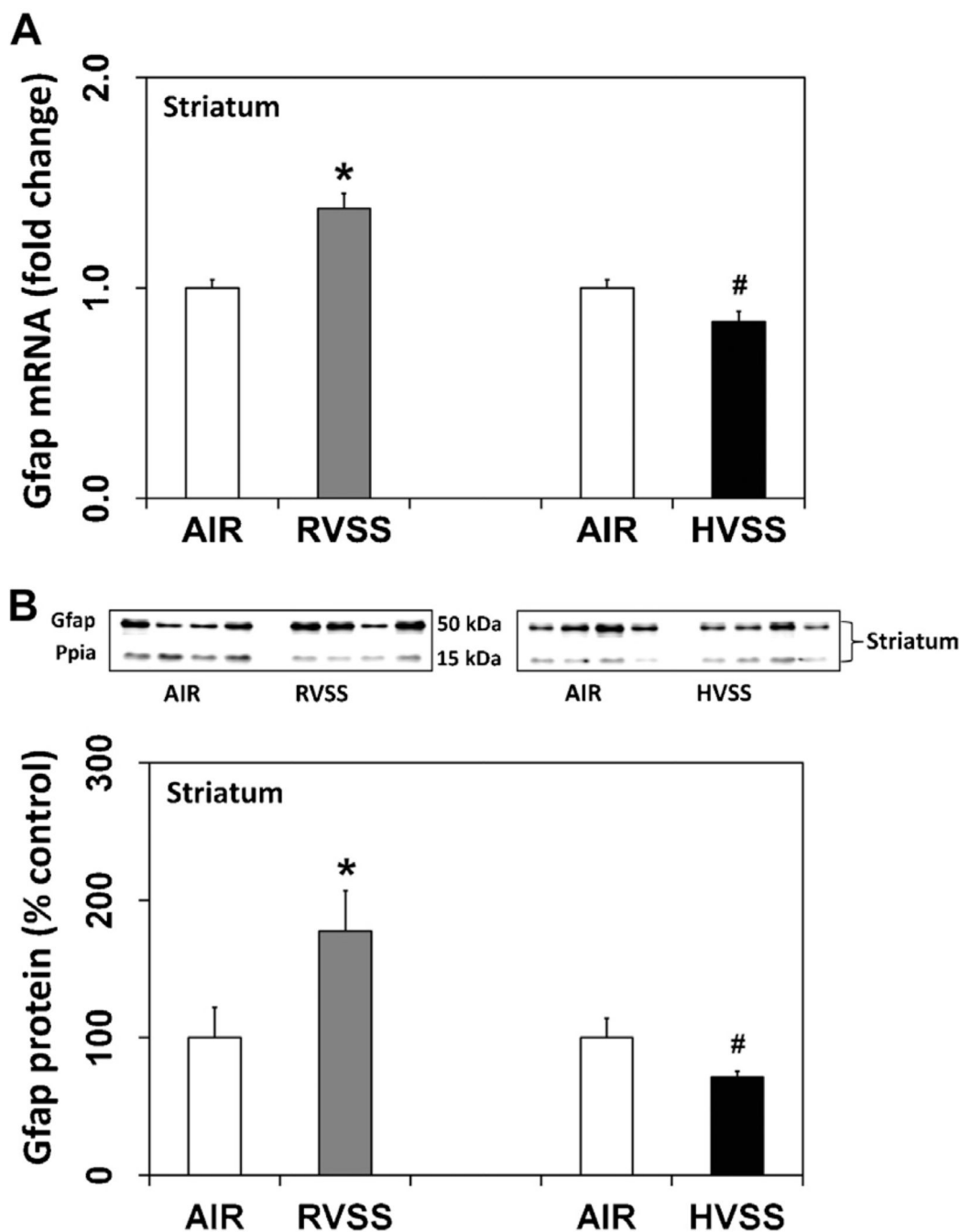


Fig. 8. Effect of RVSS and HVSS fume particulates on Gfap gene expression in the striatum. Rats were exposed by whole-body inhalation (40 mg/m^3 ; $3 \text{ h/day} \times 5 \text{ d/week} \times 2 \text{ weeks}$; for a total of 10 days) to fume particulates generated by gas-metal arc-stainless steel (GMA-SS) welding at standard/regular voltage (25 V; RVSS) or at high voltage (30 V; HVSS). (A) At 1 day post-exposure, the expression of Gfap mRNA in the STR was assayed TaqMan[®] real-time PCR. Following normalization to the endogenous control beta actin (Actb), the values are expressed as fold change from air-exposed controls. Graphical representations are Mean

\pm SE ($n = 6/\text{group}$). (B) At 1 day post-exposure, the expression of Gfap protein in the STR was determined by immunoblot analysis. Following normalization to the endogenous control cyclophilin A (Ppia), the values are expressed as percent of air-exposed controls. Graphical representations are Mean \pm SE ($n = 4/\text{group}$). * indicates significant change from corresponding air-exposed control ($P < 0.05$). # indicates significantly different from RVSS group.

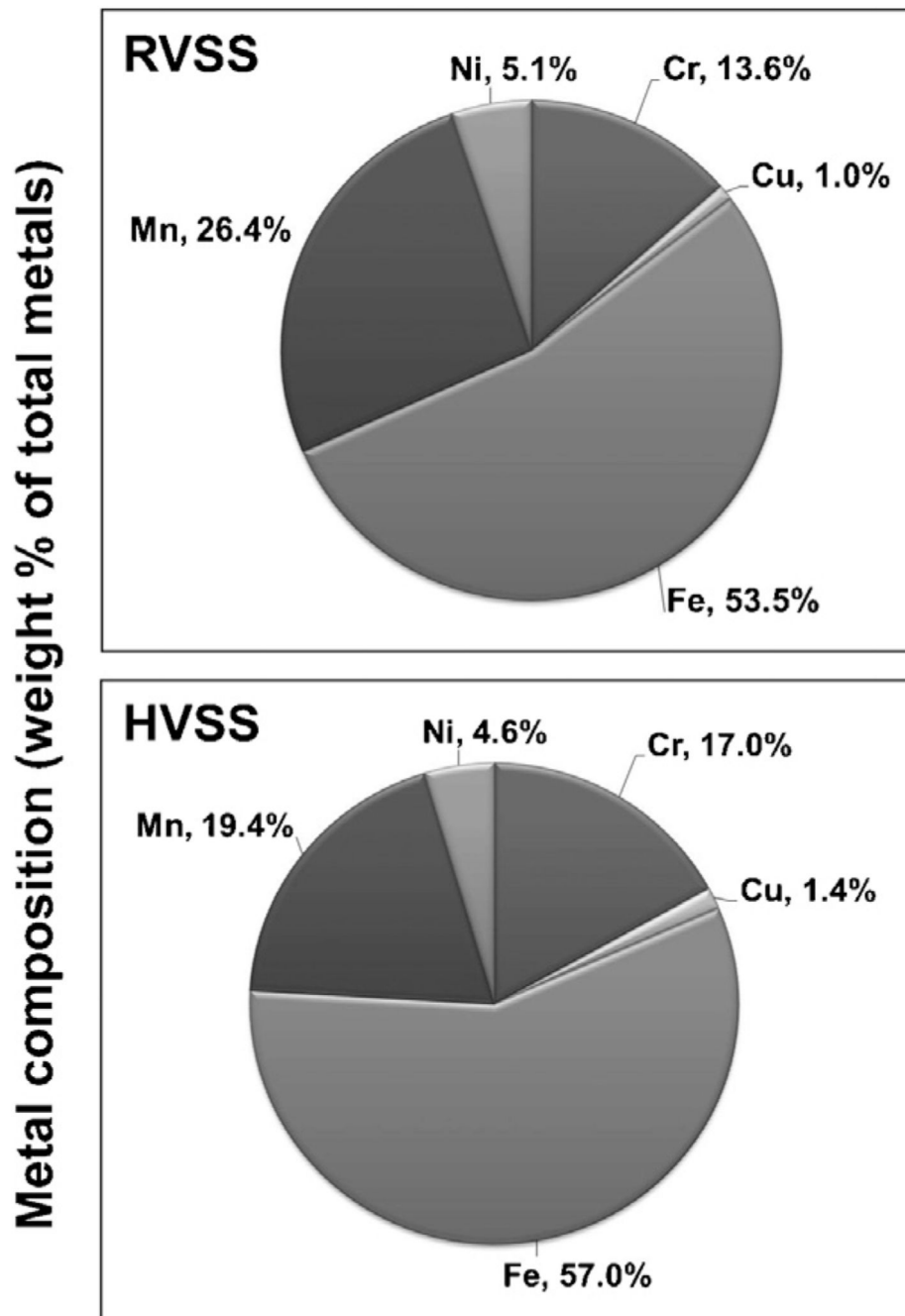


Fig. 9. Elemental composition of WF particulates generated by RVSS and HVSS welding. RVSS and HVSS fume particulates were collected on to PVC filters ($n = 4$ for each fume type) and subjected to elemental analysis by ICP-AES following the NIOSH method 7300, which can detect over thirty different elements. ICP-AES analysis of the samples revealed the presence Fe, Mn, Cr, Cu and Ni as the major components (>99%) of the fume particulates. The concentration of each element was calculated as $\mu\text{g}/\text{mg}$ of total metal and the mean

concentration was determined. The weight percent of each element that composes the total metal portion of the fume was calculated and is graphically depicted.

Author Manuscript

Author Manuscript

Author Manuscript

Author Manuscript

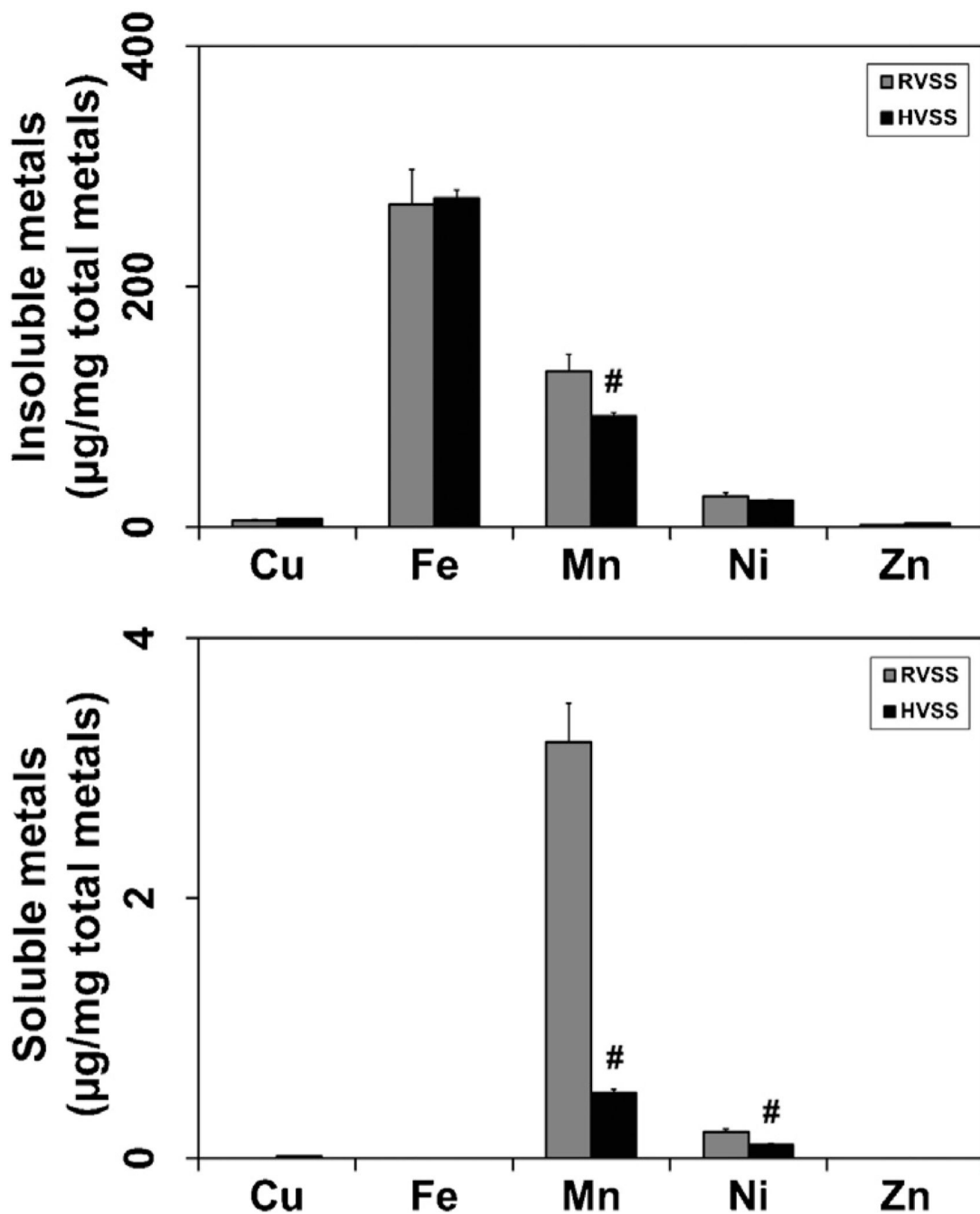


Fig. 10. Solubility of fume particulates generated by RVSS and HVSS welding. RVSS and HVSS fume particulates were collected on to PVC filters ($n = 4$ for each fume type). The particulates were suspended in distilled water, sonicated and centrifuged to obtain insoluble (pellet) and soluble (supernatant) fractions. The pellet and supernatant were subject to elemental analysis by ICP-AES following the NIOSH method 7300 to determine the elemental composition of the insoluble and soluble fractions. Fe, Mn, Ni and Cu made up the major composition (>99%) of the two fractions. The concentration of each element was

calculated as $\mu\text{g}/\text{mg}$ total metal. Graphical representations are $\text{Mean} \pm \text{SE}$ ($n = 4/\text{group}$). # indicates significantly different from RVSS group.

Author Manuscript

Author Manuscript

Author Manuscript

Author Manuscript

Table 1

Parameters for gas metal arc welding at regular and high voltage conditions.

	Regular voltage (RVSS)	High voltage (HVSS)
Weld process	Gas–metal arc welding (GMAW)	Gas–metal arc welding (GMAW)
Wire/electrode	Blue Max E308LSi (stainless steel)	Blue Max E308LSi (stainless steel)
Weld base plate	A36 Carbon steel plate	A36 Carbon steel plate
Wire feed rate	300 in/min	300 in/min
Voltage	25 V	30 V
Current	200 A	200 A
Shielding gas	Ar/CO ₂ (95:5)	Ar/CO ₂ (95:5)
Gas flow rate	20 l/min	20 l/min

Author Manuscript

Author Manuscript

Author Manuscript

Author Manuscript

Table 2

Characteristics of welding fume particulates generated at regular and high voltage.

	Regular voltage (RVSS)	High voltage (HVSS)
Particle morphology	Chain-like aggregates	Chain-like aggregates
Particle size, MMAD (GSD)	0.39 μm (1.65)	0.36 μm (1.59)
Major elements (Wt%)		
Fe	53.5 \pm 5.7	57.0 \pm 1.5
Mn	26.4 \pm 2.8	19.4 \pm 0.6 ^a
Cr	13.6 \pm 3.0	17.0 \pm 0.6
Ratio of Fe:Mn	2:1	3:1 ^a
Ratio of Fe:Cr	4:1	4:1

Particle morphology was determined from SEM photomicrographs depicted in Fig. 2. Particle size distribution was determined in the exposure chamber by using Micro-Orifice Uniform Deposit Impactor (MOUDI) and Nano-MOUDI. Elemental analysis was performed by ICP-AES and fume content of major metals is presented as weight % of total metals. Values are Mean \pm S.E. ($n = 4$; fume samples were collected at 30 min intervals).

MMAD (GSD), mass median aerodynamic diameter (geometric standard deviation); RVSS, regular voltage stainless steel fume particulates; HVSS, high voltage stainless steel fume particulates.

^aSignificantly different from corresponding value in RVSS fumes.